Development of an Er–Ni liquid alloy ion source

L. C. Chao and A. J. Steckl[a)]
Nanoelectronics Laboratory, University of Cincinnati, Cincinnati, Ohio 45221-0030

(Received 4 November 1998; accepted 19 February 1999)

We have developed a procedure for the fabrication of Er–Ni liquid alloy ion sources. The source is tested and analyzed in a MicroBeam 150 focused ion beam system. Our experimental results show that an Er^{2+} target current of 95–100 pA was produced, representing 50% of the total target current. The ion emission current–voltage slope is ~36 μA/kV. Source lifetimes are generally larger than 20 h. The alloy oxidizes quickly once it is exposed to air. This must be minimized to ensure proper source performance. © *1999 American Vacuum Society.* [S0734-211X(99)04303-6]

I. INTRODUCTION

Erbium-doped semiconductor materials have drawn increasing attention during the last ten years. This is due to the Er^{3+} emission at 1.54 μm, a standard telecommunication wavelength. Visible or infrared emission has been obtained from a variety of erbium-doped materials, such as Si,[1] SiC,[2] GaN,[3] GaAs,[4] oxide glasses,[5] and ceramic thin films.[6] Erbium is added to those materials during growth or by ion implantation. Waveguides, lasers, and light emitting diodes have been fabricated by using traditional lithography techniques.[7–9] An alternative method of fabricating the optoelectronic devices and future optoelectronic integrated circuits (OEICs) is using focused ion beam (FIB) implantation and/or micromilling. FIB technology is a maskless and resistless particle beam process, which can be applied with great versatility to the fabrication of optoelectronic devices. FIB microfabrication and nanofabrication can be utilized to reduce the complexity required of conventional OEIC fabrication technology (in particular lithography, etching, and implantation), which has to satisfy various requirements for different components fabricated on the same substrate.[10]

The success of FIB technology is primarily due to the exploitation of liquid metal ion sources (LMISs).[11,12] Er has a high melting point (1529 °C) and a high vapor pressure at its melting point (≈1 Torr), making it unsuitable for an elemental LMIS. Instead, it must be made in the form of a liquid alloy ion source (LAIS) by combining with another material in order to lower the melting point and, hopefully, a much lower vapor pressure. One attractive candidate which we have investigated for this purpose is the Er–Ni alloy. Figure 1 shows the phase diagram of the Er–Ni binary system.[13] From the diagram one can observe that a mixture of erbium and nickel at an atomic percent ratio of 69(Er):31(Ni) produces a eutectic binary alloy with a melting point of 765 °C.

II. EXPERIMENT

The source is made by using a 250 μm diam tungsten wire. The wire is twisted around a 0.125 in. outer diameter Al_2O_3 rod in order to be fitted into the ion gun module of a MicroBeam 150 FIB system. Another tungsten wire is wrapped around the first wire's shank to form a reservoir. The tip is mechanically polished and then electrochemically etched in a NaOH solution until the end radius is approximately 10 μm. The source is wetted with Er–Ni alloy in a separate vacuum system. The alloy was prepared by mixing erbium and nickel powders at an atomic ratio of Er(69):Ni(31). The mixed powder was put into an Al_2O_3 crucible that can be heated to temperatures above 1800 °C by a tungsten filament. Before dipping the tip into the crucible, the crucible was heated to 1800 °C for 2 min to ensure proper mixing. After the alloy was in its molten state, the tip was dipped into the crucible for 30 s and then retracted. A puddle of the alloy should form on the reservoir. The source is tested *in situ* by applying appropriate voltage and heating current to the source.

After the preliminary test, the source is then transferred to a MicroBeam 150 FIB system. The MicroBeam 150 FIB system is a 150 kV two-lens system which incorporates an $E \times B$ mass separator with a sensitivity of $m/\Delta m = 50$. The Er–Ni source was positioned at 3.5 mm upstream of a Wehnelt electrode which has an aperture of 3 mm in diameter. The extractor electrode was positioned 25 mm downstream of the Wehnelt electrode, which has an aperture of 1.85 mm in diameter. The extractor voltage V_E is applied between the extractor electrode and the source. The Wehnelt electrode was biased at positive 1.1 kV relative to the source. An automatic source stabilization software program to maintain steady emission adjusted the Wehnelt electrode voltage. During the experiment, the variation of the Wehnelt electrode voltage was less than 20 V. The current–voltage ($I-V$) dependence of the Er–Ni LAIS was obtained by changing V_E from 6 to 8 kV. The target current was collected by a Faraday cup in the target chamber. During the experiment, the total acceleration voltage was maintained at 30 kV.

III. RESULTS

Figure 2 shows the $I-V$ dependence of an Er–Ni LAIS. Emission current is first obtained at $V_E = 6.7$ kV. The emission is increased by ramping up V_E to 8 kV. This is followed by ramping down V_E until the emission is extinguished at just below 6.5 kV. The $I-V$ slopes for ramp up and ramp down are roughly equal, with a value of 36 μA/kV being

a)Electronic mail: a.steckl@uc.edu

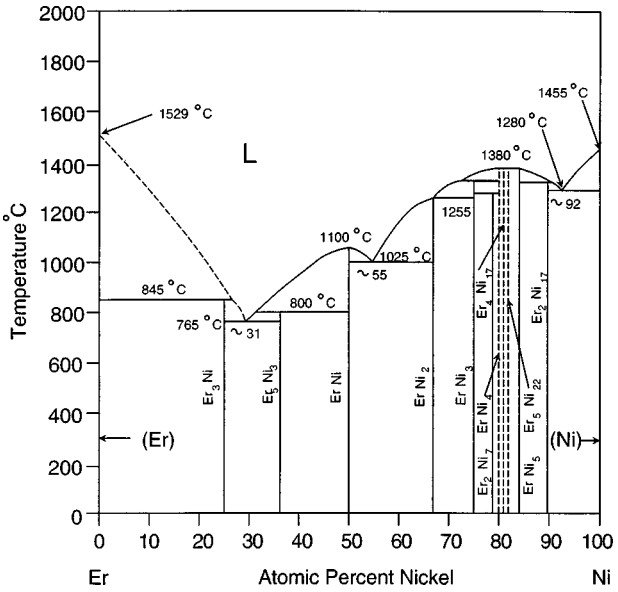

FIG. 1. Phase diagram of the Er–Ni system.

obtained by first order curve fitting. This value is about the same as results obtained by other groups utilizing similar needle-type LMIS[14–17] design.

The mass spectrum of the Er–Ni LAIS was obtained by sweeping the electric field of the $E \times B$ filter from 0 to 70 V while the magnetic field was driven by a direct current of 0.75 A. The voltage is then converted to the m/q ratio by comparing with a previously characterized Au–Si LAIS. Figure 3 shows the mass spectrum of the Er–Ni LAIS with the extractor voltage set at 7.5 kV and the total ion emission current of 15 μA. The data in Fig. 3 indicate that doubly charged erbium ions (Er^{2+}) represent the single largest component of the beam (95 pA), producing approximately 50% of the total target current of 190 pA. Utilizing the system's

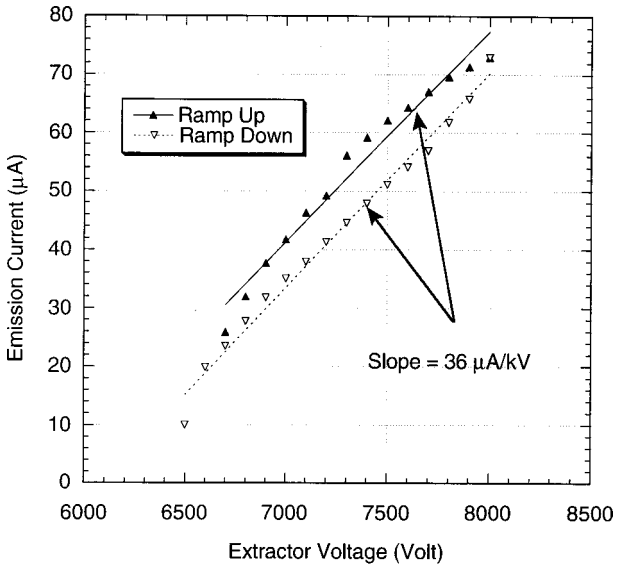

FIG. 2. Current–voltage dependence of the Er–Ni LAIS operated with a heater current of 6.9 A.

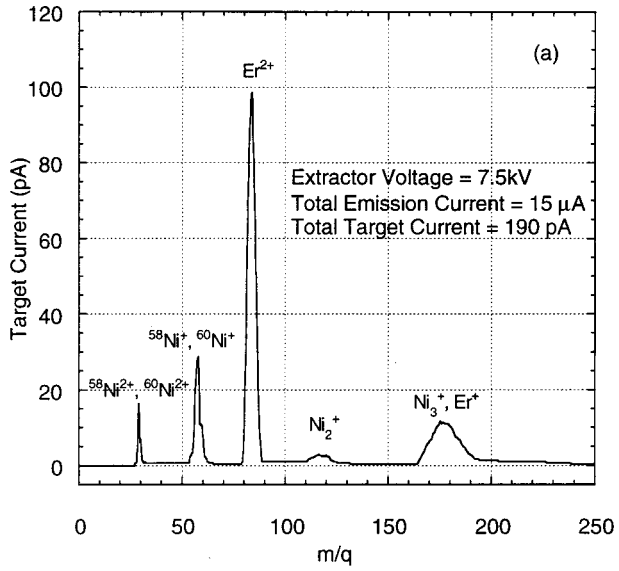

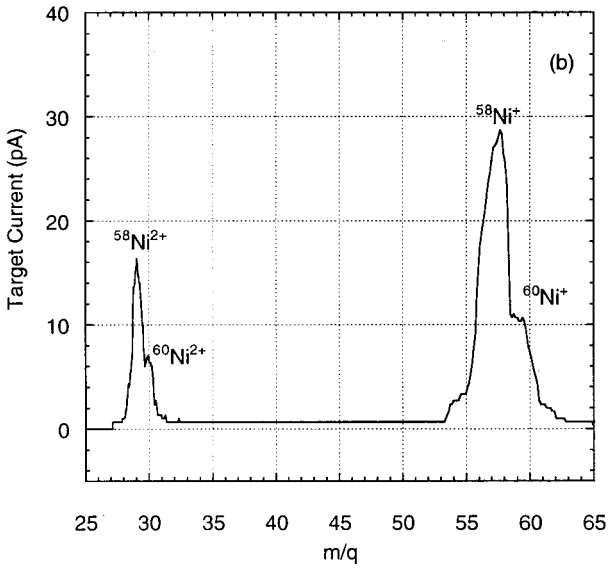

FIG. 3. Mass spectrum of the target current from the Er–Ni LAIS: (a) full spectrum showing the Ni and Er ion beam components; (b) selected spectrum showing the contributions from the ^{58}Ni and ^{60}Ni isotopes.

mass filtering resolution, the ion beam components associated with the two main nickel isotopes Ni^{58} and Ni^{60} can be distinguished. Their respective ion currents are present in the same ratio as their natural abundance ($\sim$2.5). Because of their much higher masses, the main individual isotopes of Er (with mass numbers 166, 167, 168, and 170) were not observed.

An optimum source operation temperature was obtained experimentally to minimize the degrading of the background pressure while maintaining the source stability. In our experiment, the optimum heating current was 6.9 A. The background pressure was 1.2×10^{-7} Torr before the heating current was applied to the source. After 3 h of operation, it increased to 1.5×10^{-7} Torr. This indicates that the vapor pressure of the alloy under this heating current does not sig-

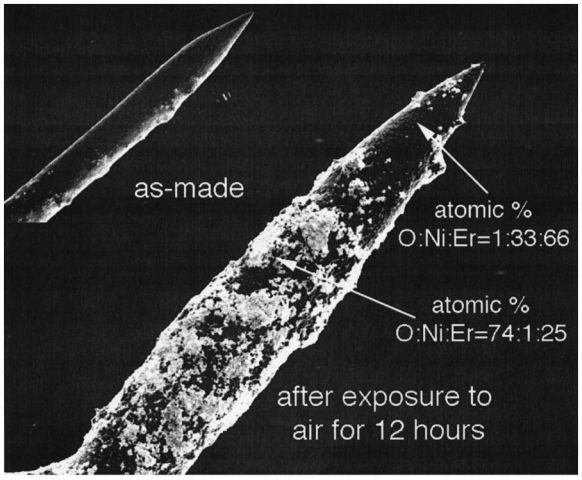

FIG. 4. SEM microphotographs of an Er–Ni LAIS before and after 12 h exposure to air.

nificantly deteriorate the background pressure.

Figure 4 shows a scanning electron micrograph (SEM) of an Er–Ni LAIS before and after being exposed to air for 12 h. The heavy formation of oxides on the surface of the tip is observed. Energy dispersive x-ray spectroscopy (EDX) shows that the oxide has an atomic percent ratio of O:Ni:Er=74:1:25, while the ''clean'' area has an atomic percent ration of O:Ni:Er=1:33:66. EDX results also show that the residual alloy in the crucible has a composition of Ni:Er=32:68 at. % which is very close to the originally mixed ratio. The formation of the oxides degrades the source stability and shortens its lifetime. Contamination must be therefore minimized to maintain adequate source performance.

IV. CONCLUSIONS AND SUMMARY

We have developed a procedure for the fabrication of Er–Ni liquid alloy ion sources. The largest emission peak is Er^{2+} which represents 50% of the total target current. The $I-V$ characteristics show that the source can readily be incorporated into a modern focused ion beam system for high resolution maskless erbium implantation. The vapor pressure of the source at its working temperature is not a serious problem to the background pressure. The alloy oxidizes quickly once it is exposed to air. This contamination must be minimized to ensure proper source performance.

ACKNOWLEDGMENTS

This work was supported by BMDO/ARO and MRL contracts.

[1]Y.-H. Xie, E. A. Fitzgerald, and Y. J. Mii, J. Appl. Phys. **70**, 3223 (1991).
[2]A. J. Steckl, J. Deverajan, W. J. Choyke, R. P. Devaty, M. Yoganathan, and S. W. Novak, J. Electron. Mater. **25**, 869 (1996).
[3]A. J. Steckl and R. Birkhahn, Appl. Phys. Lett. **73**, 1700 (1998).
[4]T. D. Culp, U. Hommerich, J. M. Redwing, T. F. Kuech, and K. L. Bray, J. Appl. Phys. **82**, 368 (1997).
[5]F. Priolo, G. Franzo, S. Coffa, A. Polman, E. Snoeks, G. N. van den Hoven, S. Libertino, S. Lombardo, S. U. Campisano, and A. Carnera, Nucl. Instrum. Methods Phys. Res. B **116**, 77 (1996).
[6]G. N. van den Hoven, E. Snoeks, A. Polman, C. van Dam, J. W. M. van Uffelen, and M. K. Smit, J. Appl. Phys. **79**, 1258 (1996).
[7]A. Steckl, M. Garter, R. Birkhahn, and J. Scofield, Appl. Phys. Lett. **73**, 2450 (1998).
[8]K. Hattori, T. Kitagawa, and Y. Ohmori, J. Appl. Phys. **79**, 1238 (1996).
[9]G. Franzo, F. Priolo, S. Coffa, A. Polman, and A. Carnera, Nucl. Instrum. Methods Phys. Res. B **96**, 374 (1995).
[10]A. J. Steckl, Proceedings of Advanced Workshop on Frontiers in Electronics, Tenerife, Spain, IEEE Cat. No. 97TH8292, 47 (Jan. 1997).
[11]J. Orloff, Rev. Sci. Instrum. **64**, 1105 (1993).
[12]J. Melngailis, J. Vac. Sci. Technol. B **5**, 469 (1987).
[13]*Binary Alloy Phase Diagrams*, edited by T. B. Massalski (ASM International, Materials Park, OH, 1990).
[14]S. D. Papadopoulos, Ph.D. thesis, Oxford University, 1986.
[15]D. R. Kingham and L. W. Swanson, Appl. Phys. A: Solids Surf. **34**, 123 (1984).
[16]G. L. R. Mair, Vacuum **36**, 847 (1986).
[17]A. Wagner and T. M. Hall, J. Vac. Sci. Technol. **10**, 1871 (1977).